Assessment of earthquake resistant techniques in the out-of-plane behaviour of stone masonry walls

Influência de técnicas sismo-resistentes no comportamento para fora do plano de paredes de alvenaria de pedra

Antonio Murano
Javier Ortega
Graça Vasconcelos
Hugo Rodrigues

Abstract

FE method is a useful and powerful tool widely applied to the structural analysis of masonry constructions. One of the main challenges related to the numerical simulations is the use of adequate constitutive materials models able to replicate, in an accurate way, the non-linear behaviour of masonry. Thus, the experimental characterization of the masonry can allow overcoming the uncertainties regarding the material mechanical properties.

Macro-modelling is a very popular FE approach that approximates masonry as a homogeneous isotropic continuum, in order to obtain simpler and larger meshes, because the model does not have to describe the internal structure of masonry. Hence, macro-modelling provides a good balance between accuracy and efficiency.

This work presents a methodology applied to the calibration of two numerical macro-models reproducing the OOP response of reduced scale (1:2) U-shaped stone masonry walls built with earthquake resistant techniques embedded at the corners (WALL 1 – steel ties and WALL 2 – timber lath beams), which were previously tested experimentally by using an airbag to simulate the seismic load.

The outcomes, provided by this work, represent a useful contribution in order to assess the effectiveness of the macro-model approach for the analysis of masonry buildings.

Resumo

Um dos desafios principais do uso do método de elementos finitos (FE) para a análise estrutural de construções de alvenaria é o uso de modelos constitutivos que sejam capazes de replicar apropriadamente o comportamento não linear da alvenaria. A caracterização experimental da alvenaria permite diminuir as incertezas relacionadas com as propriedades mecânicas do material. Este trabalho apresenta a metodologia aplicada para a calibração de dois modelos FE que reproduzem duas paredes de alvenaria de pedra em forma de U ensaiadas no laboratório. Os modelos seguem uma abordagem macro-modelo. As paredes ensaiadas foram construídas com dois dispositivos sismorresistentes tradicionais inseridos nos cunhais, nomeadamente tirantes de aço (WALL 1) e vigas de madeira (WALL 2), e foram ensaiadas fora do plano mediante o uso de airbags para a simulação da carga sísmica. Os resultados deste trabalho contribuem para avaliar a eficácia da abordagem macromodelo para a análise estrutural de edifícios de alvenaria.

Antonio Murano

PhD Student
University of Minho
Guimarães, Portugal
antoniomurano1987@gmail.com

Javier Ortega

Postdoc Researcher
University of Minho
Guimarães, Portugal
javier.ortega@civil.uminho.pt

Graça Vasconcelos

Assistant Professor
University of Minho
Guimarães, Portugal
graca@civil.uminho.pt

Hugo Rodrigues

Assistant Professor
Polytechnic Institute of Leiria
Leiria, Portugal
hugo.f.rodrigues@ipleiria.pt

1 Introduction

Due to its heterogeneity and its complexity in terms of material properties, several numerical techniques have been deployed by researchers over time, in order to adequately deal with a complex task such as masonry structures modelling [1].

Two are the main FE-based approaches to model masonry intended as a composite material [2]:
- Equivalent continuum idealization (macro-modelling);
- Equivalent discontinuous idealization (micro-modelling and meso-modelling).

The numerical analyses presented in this paper have been carried out using a macro-modelling approach, which is typical of practice-oriented engineering activities. Masonry is approximated as a homogeneous isotropic continuum. Therefore, no detailed simulation of the interaction between stone units and mortar is provided [3].

The continuum parameters must be determined by means of tests on specimens of sufficiently large size subjected to homogeneous states of stress.

This approach has significant practical advantages related to the fact that FE meshes are simpler and with a larger size because they do not have to accurately describe the internal structure of masonry. Hence, macro-modeling provides a good compromise when a balance between accuracy and computational efficiency is required.

1.1 Objective and methodology of the present work

This paper presents the approach followed in order to calibrate a numerical model starting from the outcomes of experimental campaigns previously carried out in order to assess the out-of-plane (OOP) performances of stone masonry walls built with and without earthquake resistant techniques.

The reference experimental data used during the calibration procedure are provided in Maccarini *et al.* (2018 [4]) and in Murano *et al.* (2018) [5]. The work carried out by Maccarini *et al.* (2018) [4], addressing the OOP characterization of plain walls, has been further extended in order to evaluate the influence of different earthquake resisting techniques on the out-of-plane response of stone masonry walls. To this end, two U-shaped reduced scale stone masonry prototypes (1:2) were built with earthquake-resistant techniques, namely WALL 1 (steel ties) and WALL 2 (timber lath beams) [5].

In order to enable a direct comparison with the results related to the plain wall (WALL 0, see [4]), the same geometry for the wall prototypes, testing setup and instrumentation were used.

Once the construction of the reduced scale stone masonry walls was completed, their mechanical and dynamic characterization was carried out by means of sonic tests and dynamic identification tests respectively [5]. Preliminarily, an accurate geometrical characterization and an assessment of the mortar properties was conducted in order to monitor the overall quality of the construction process and, at the same time, in order to use the data to empirically evaluate the prototypes density.

The out-of-plane performance of the stone masonry walls was assessed using an airbag, which simulated the horizontal seismic load acting on the rear surface of the tested prototype. A supporting steel frame was placed between the reinforced concrete reaction wall of the laboratory and the airbag. The out-of-plane test was carried out under displacement control. The control point was located at the top of the frontal wall at its mid-span where the highest displacement was expected. The monitoring of the displacements of the frontal wall during the out-of-plane test was carried out using linear variable differential transducers (LVDTs). Figura 1 depicts a comparison among the cyclic envelope related to reinforced (WALL 1/WALL 2) and unreinforced (WALL 0) stone masonry wall prototypes tested using same cyclic procedure, characterized by similar masonry bond and similar stone/mortar mechanical properties.
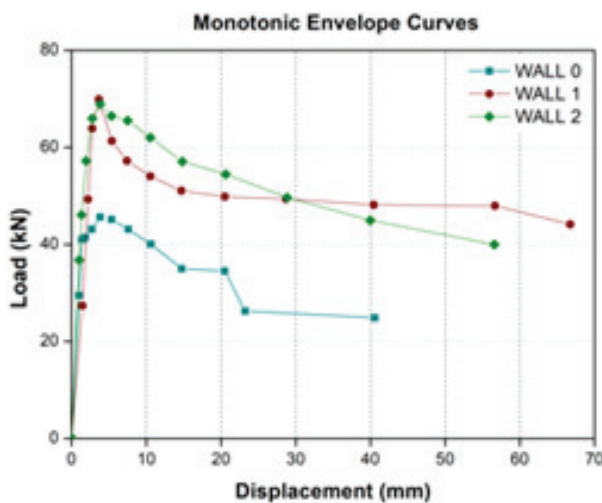

Figure 1   Monotonic envelope curves WALL 0, WALL 1, WALL 2

Once the OOP characterization of the prototypes was completed, numerical simulations were carried out in order to compare the experimental envelope and the numerical capacity curves defined by means of static nonlinear analysis (pushover method) assessing, at the same time, the effectiveness of the applied modelling approach (macro-model).

2   Numerical simulation

A methodology aimed at the calibration of a numerical model, based on the experimental data collected before the out-of-plane (OOP) airbag test, is herein presented. Successively, a pushover analysis reproducing the OOP test has been carried out, in order to compare the numerical and experimental results. Further considerations, have been realized pointing out, where it was possible, the main differences in terms of crack pattern and load capacity regarding reinforced and unreinforced prototypes.

2.1   Finite element model

The numerical model of the wall was constructed with DIANA software (TNO 2106) [6] using twenty-node tetrahedron solid 3D elements (CHX60). Plane quadrilateral interface elements (CQ48I) in a three-dimensional configuration were applied in order to reproduce the connection between the concrete base of the prototypes and the strong floor of the laboratory. Wall and concrete base are considered to be fully connected. Steel and timber reinforcing elements were modelled using tetrahedron solid 3D elements (CHX60); the reinforcing elements were subtracted to the model's geometry by means of Boolean operation.

Moreover, an adequate connection among the nodes of the embedded elements (CL18B) and the solid elements (CHX60) mesh must be ensured. Both steel and timber elements have been analysed assuming a linear elastic behaviour. Steel Young modulus was assumed equal to 210,000 MPa, whereas 7800 kg/m³ and 0.3 are the selected values for density and Poisson ratio respectively. Timber Young modulus was assumed equal to 10,000 MPa; timber density and Poisson ratio are equal to 600 kg/m³ and 0.2 respectively [7] [8]. The cross-section dimensions of the reinforced elements have been presented in section Murano *et al.* (2019) [5].

Figure 2 shows the reference models prepared. In order to have a good representation of the strain and stress distribution, the overall size of the finite elements mesh is equal to 0.10 m. On the other hand, the mesh size for the reinforcing elements was reduced according to their geometrical characteristics. In the steel reinforcements, the mesh has been generated so that at least three finite elements defined the thickness of the solid, whereas the mesh size in the timber elements is equal to 0.05 m.

Mesh configuration
WALL 0

Mesh configuration
WALL 1

Mesh configuration
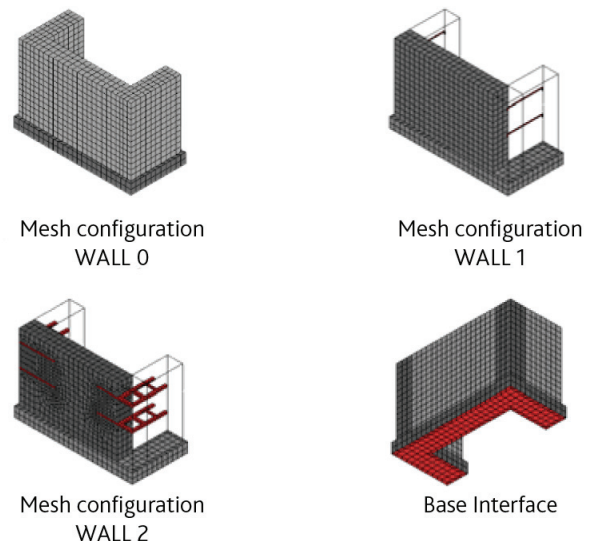WALL 2

Base Interface

Figure 2   Reference model and embedded elements

The material model adopted to represent the non-linear behaviour of the stone masonry is a standard isotropic Total Strain Rotating Crack Model (TSRM) [6]. The model describes the tensile and compressive behaviour of the material with one stress-strain relationship and assumes that the crack direction rotates with the principal strain axes. Moreover, it is very well suited for analyses predominantly governed by cracking or crushing of the material [9].

The non-linear behaviour of the material in tension is simulated by means of an exponential softening function, whereas the compressive function selected to model the crushing behaviour is parabolic [6].

2.2 Calibration of the numerical model

The calibration process followed three steps:
- Reference material elastic properties were estimated based on the results of the sonic tests (see [4] and [5]);
- The properties were further adjusted based on the comparison between the numerical and experimental frequencies;
- The nonlinear material properties were adjusted based on the comparison of the force displacement envelope obtained in the out-of-plane experimental test with the nonlinear static (pushover) analysis performed on the numerical model.

A linear elastic behaviour was assumed for the concrete base, with a modulus of elasticity and a Poisson's ratio equal to 31 GPa and 0.2 respectively.

The adjustment of the interface elastic properties was based on the initial stiffness of the base shear-out-of-plane displacement curve obtained on the LVDT placed at the inferior corner (WALL 1) and at the mid-span of the concrete base (WALL 2), see [5]. The calibration of the numerical model was done by changing the values of the normal and tangential stiffness of the elastic interface elements in order to obtain values of natural frequencies and mode shapes compatible with the experimental results.

WALL 0 tangential stiffness in both directions (X and Y) was set equal to 3.97×10^8 N/m³; the stiffness in the normal direction was equal to 9.92×10^8 N/m³ [4].

At the end of the calibration phase related to WALL 1, an interface tangential stiffness of 2.47×10^8 N/m³ was obtained for both directions. The normal stiffness was set at 6.175×10^8 N/m³. In WALL 2 calibration, an interface tangential stiffness of 2.57×10^8 N/m³ was obtained, whereas the stiffness in the normal direction was set at 6.40×10^8 N/m³. Once this calibration stage was completed, a preliminary pushover analysis was carried out.

The comparison between the resulting capacity curve and the experimental envelope made it possible to further modify other materials mechanical properties, such as Young modulus and tensile strength, in order to have a more accurate approximation regarding the linear behaviour and the peak load. Therefore, in both walls, the experimental value of the Young modulus underwent a 20% reduction and, consequently, all the materials properties were defined based on the update parameter.

The compressive strength was assumed using the range proposed by Tomaževič (1999) [10], where it can be estimated as a function of the modulus of elasticity previously updated: $E\alpha f_c$, where α ranges from 200 to 1000. A value of 1000 was assumed for this work. The tensile strength (f_t) was initially established at 10% of the compressive strength, and then reduced up to 2%, 3% and 2.5% for WALL 0, WALL 1 and WALL 2 respectively after calibration with the experimental tests. The compressive fracture energy was calculated by multiplying the compressive strength by a ductility index of

1.6 mm, based on recommendations of Lourenço (2009) [3]. The mode I fracture energy was set equal to 12 N/m, following the same set of recommendations.

Table 1 summarizes linear and non-linear properties obtained after the calibration procedure.

Table 1 Linear and non-linear material properties after calibration procedure

	Linear material properties			Non-linear material properties			
	E (MPa)	ν	ρ (kg/m³)	f_c (MPa)	G_{fc} (N/m)	f_t (MPa)	G_{f_t} (N/m)
WALL 0	3600	0.39	2495	3.60	5760	0.072	12
WALL 1	2450	0.34	2513	2.45	3917	0.073	12
WALL 2	2974	0.37	2482	2.97	4759	0.074	12

Table 2 compares the numerical frequencies, obtained numerically by means of an eigenvalue analysis with updated parameters, to the experimental ones. A modal participation in the out-of-plane direction of 75.55% and 75.85% were calculated in WALL 1 and WALL 2 respectively. Furthermore, WALL 0 first mode frequency was equal to 25.847 Hz, with a modal participation in the out-of-plane direction of 74.68% (Maccarini *et al.*, 2018 [4], section 5.2.1). The frequency related to unreinforced wall are slightly higher than the reinforced wall, but the mode shapes are the same (see Table 2).

The validation of the frequencies was calculated based on the Modal Assurance Criterion (MAC). An average value of 0.98 for the first mode, 0.91 for the second mode and 0.90 for the third mode were calculated regarding WALL 1. MAC values related to WALL 2 are 0.84 (first mode), 0.86 (second mode), 0.72 (third mode).

Despite the asymmetry characterizing the experimental mode shapes, which slightly differ from the numerical results, it is possible to conclude that the MAC obtained values validate the models realized.
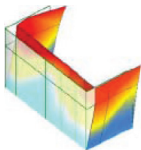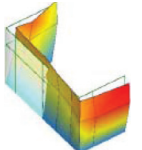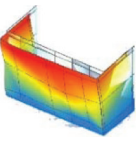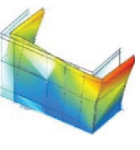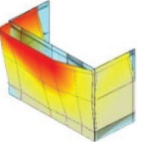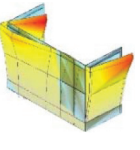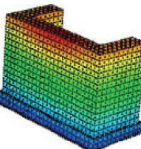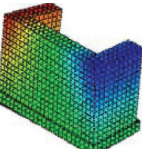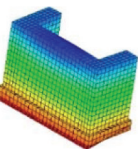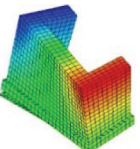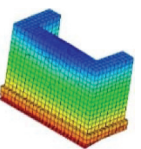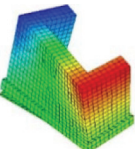
2.3 Numerical vs. experimental results

The numerical model was analysed by means of nonlinear static (pushover) analysis, considering the boundary and loading conditions adopted in the experimental tests [5]. The vertical actions applied to the model were the self-weight of the structure and the additional uniformly distributed load on the transversal walls (10 kN on each side). The uniformly distributed load on the transversal walls in WALL 2 numerical model was set equal to 20 kN in order to take into account some variations in terms of load distribution detected during the testing procedure.

In order to simulate the airbag action, a uniformly distributed horizontal load was incrementally applied until collapse on the rear surface of the frontal wall.

A capacity curve, resulted from the pushover analysis, describes the response of the structure. It represents the horizontal load *versus* the

Table 2 Experimental vs. numerical mode shapes and frequencies (wall 1, wall 2 and UR wall)

Experimental results					
WALL 0		WALL 1		WALL 2	
Mode 1	Mode 2	Mode 1	Mode 2	Mode 1	Mode 2
26.70 Hz	34.85 Hz	20.60 Hz	31.25 Hz	21.29 Hz	33.40 Hz
Numerical results					
WALL 0		WALL 1		WALL 2	
Mode 1	Mode 2	Mode 1	Mode 2	Mode 1	Mode 2
25.85 Hz	30.87 Hz	20.27 Hz	25.15 Hz	21.01 Hz	26.30 Hz
Err (%)					
3.10	11.40	2	24	1	27
MAC					
0.94	0.80	0.98	0.91	0.84	0.86

displacement of a control point detected in the same position where the control LVDT was placed during the experimental test (top mid-span of the frontal wall, see Murano *et al.* section 4.1 [5]).

Hence, the pushover curve can be directly compared with the experimental force-displacement envelope (Figure 3).

In Figure 3 is clearly visible an accurate simulation of the elastic behaviour in all the tested prototypes (WALL 0, WALL 1 and WALL 2) up to the peak load. The numerical post-peak branch in WALL 0 differs from the experimental curve. A similar behaviour is clearly visible in WALL 1, which is characterized by a significant section

highlighting increasing displacements for relatively constant load levels (ranging from 50 to 47 kN). This trend could be representative of a sliding displacement occurred in a large portion of the front wall where the reference LVDT (control point) was placed. Therefore, the aforementioned local mechanism prevails over the global response of the prototype, in terms of data recording. On the other hand, WALL 1 numerical curve highlights a decreasing trend in terms of load capacity for increased displacement levels.

WALL 2 post-peak numerical branch is slightly closer to the trend characterizing the experimental envelop. In this case, the global
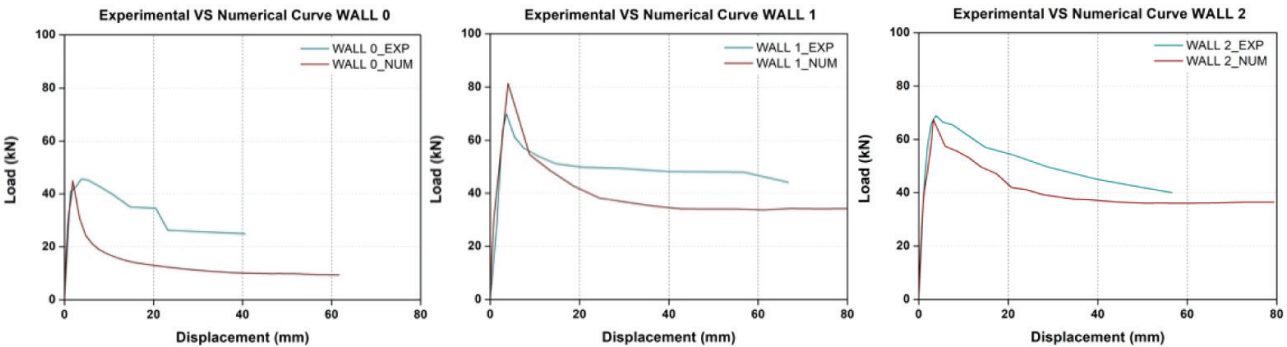

Figure 3 Experimental vs. numerical capacity curve (WALL 0, WALL 1, WALL 2)

WALL 0 – E1 front   WALL 1 – E1 front   WALL 2 – E1 front

WALL 0 – E1 rear   WALL 1 – E1 rear   WALL 2 – E1 rear
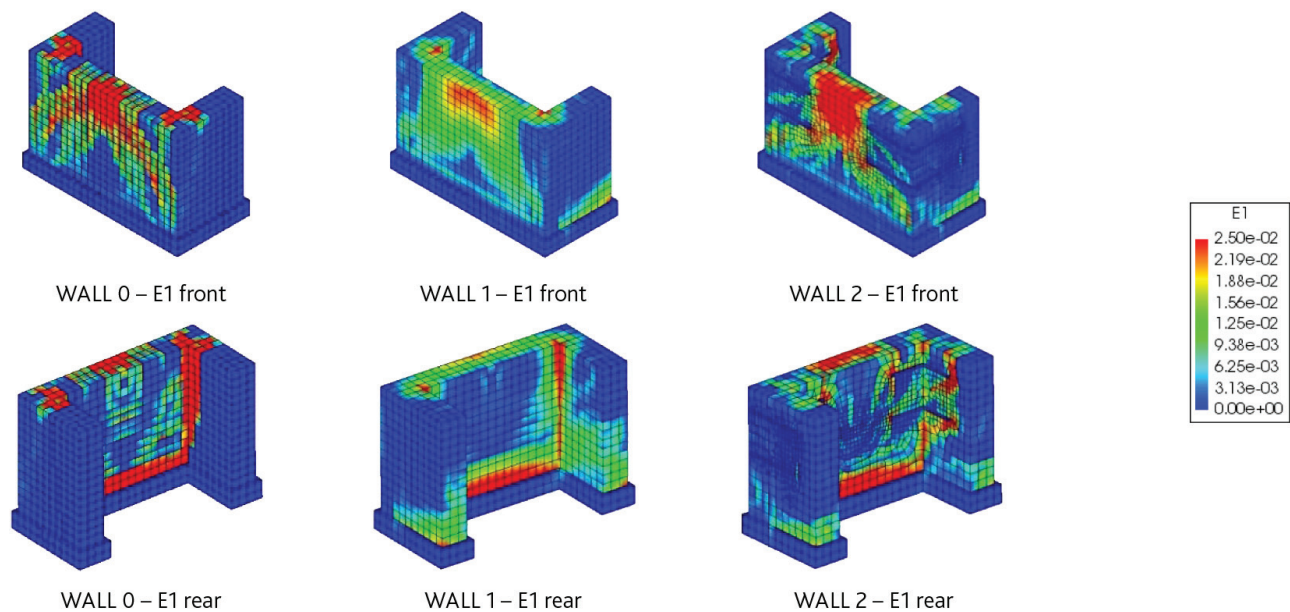
Figure 4   Maximum principal strain distribution (E1)

response of the masonry prototype subjected to horizontal load is representative of a response closer to the "ideal" one, which can be, for this reason, easier simulated using numerical methods.

The maximum load in WALL 0 numerical model (45.04 kN) is extremely close to the experimental load detected (45.64 kN). In WALL 1 numerical model the maximum load is 16% higher than experimental result (81.43 kN against 69.91 kN). On the other hand, the experimental (68.91 kN) and numerical (67.50 kN) maximum loads detected in WALL 2 are almost the same. These errors are most likely related to the uncertainties of the effective contact area between the airbag and the wall, as well as to strength degradation in the experimental tests due to the cyclic load, which was not considered in the numerical analysis.

Figure 4 presents the maximum principal strains distribution (E1) for all the tested walls, related to a level of displacement equal to 40 mm. The highest values of strain can be associated to the development of cracks.

According to the numerical models, one of the most critical areas is located at the top part of the frontal wall, at mid-span, associated with the highest displacements observed and with the bending failure of the walls. Significant strain levels can be also detected in the intersections between front and transversal walls, showing the formation of cracks that can eventually lead to the separation of the walls. This phenomenon is significant in the plain wall (WALL 0), whereas a reduction in terms of strain concentration is visible in WALL 1 and WALL 2, due to the presence of the reinforcements. Moreover, looking at WALL 2 model, it is clear that a high level of deformation characterizes the interface between timber elements and mortar joints. This trend is also confirmed by the crack pattern detected after the OOP test (see Figure 5).
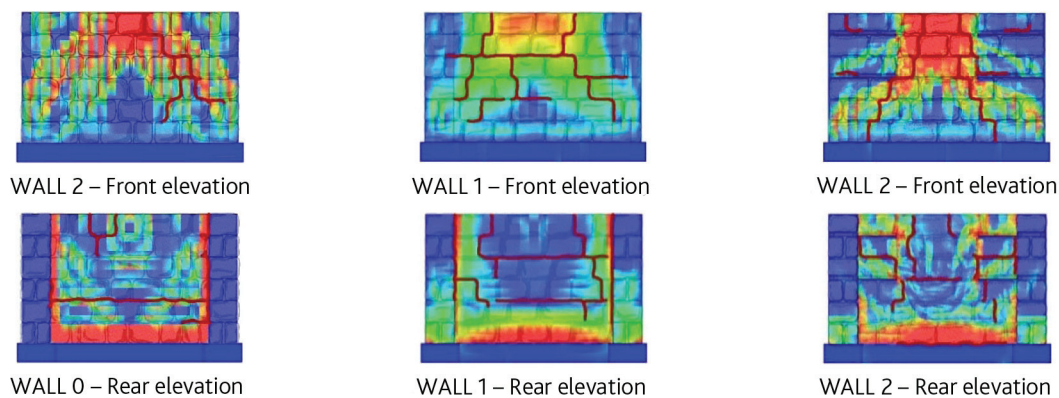

WALL 2 – Front elevation   WALL 1 – Front elevation   WALL 2 – Front elevation

WALL 0 – Rear elevation   WALL 1 – Rear elevation   WALL 2 – Rear elevation

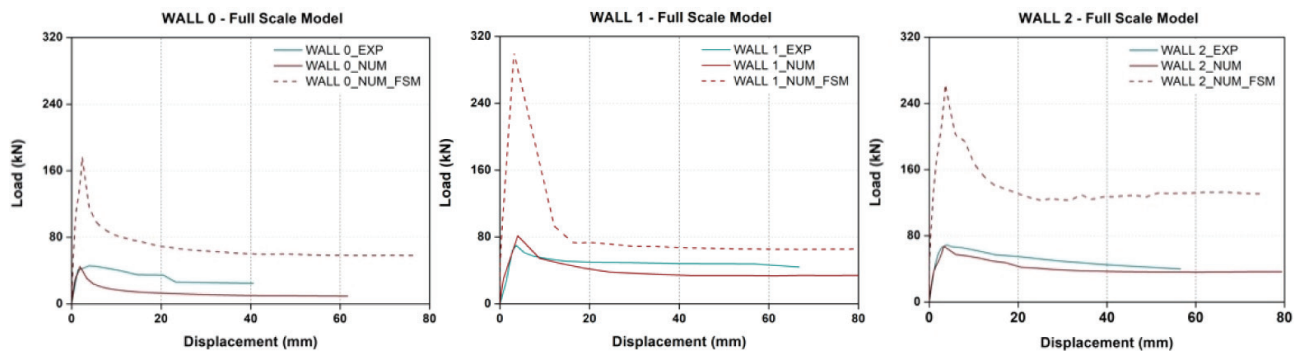**Figure 5**   Crack pattern reinforced and unreinforced prototypes

Figure 6   Numerical push-overs curves full scale models (WALL 0, WALL 1, WALL 2)

Finally, damage is also widespread at the connection between the walls and the concrete base, showing the eventual failure given by the out-of-plane rotation of the wall. This overturning damage pattern is common in buildings where there is no diaphragm action.

It should be noted that during the experimental tests, due to setup limitation, the damage pattern at the inner side of the walls could not be observed. Thus, some cracks, such as those at the base, may be closed and hidden at the end of the test, due to the self-weight of the structure.

Figure 5 compares the maximum principal strains obtained with the numerical analyses with the crack pattern observed in the experimental tests. Despite the modelling limitations and the visual limitations during the experiment, the areas of higher concentration of tensile strains are rather consistent with the crack pattern observed in the inner and outer side of the frontal wall, as well as with the cracks observed at the intersection between orthogonal walls after the test.

The experimental crack pattern in unreinforced wall is quite asymmetric. On the other hand, looking at the crack distribution in reinforced walls, it is clearly visible the result of the confinement action exerted by the reinforcing elements. Despite the occurrence a local mechanism acting on a central portion of the façade, WALL 1 shows a symmetrical distribution of the damages which can be considered an evidence of the steel reinforcement effectiveness (Figure 5).

In WALL 2, the damage distribution is governed by the reinforcements configuration, which led to the formation of inclined symmetric cracks affecting a reduced portion of façade delimited by the timber elements (Figure 5).

Numerical simulations were also performed to full scale models. To this end, WALL 0, WALL 1 and WALL 2 numerical models were scaled (2:1) with respect to the reference prototypes in order to have dimensions close to real stone masonry walls. The reference scale factors were determined according to the Cauchy law used to define small-scale models [4].
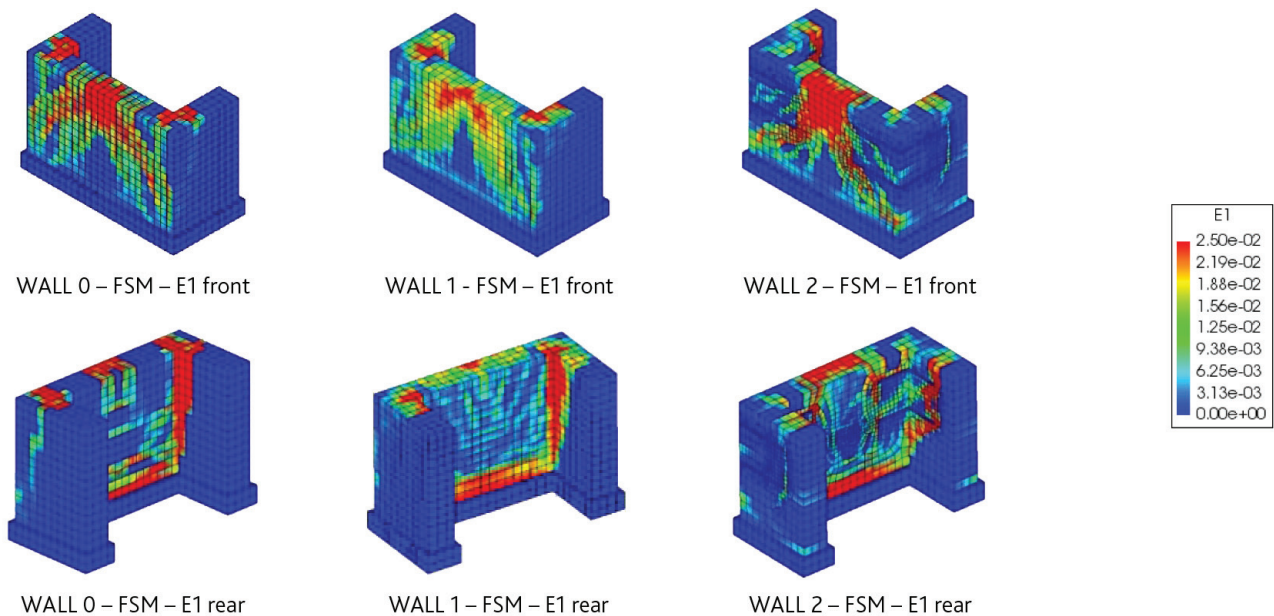

Figure 7   Maximum principal strain distribution full scale models (E1)

The variation of the scale resulted in a peak load equal to 176.42 kN, 300.80 kN and 262.80 kN in WALL 0, WALL 1 and WALL 2 respectively, which is in agreement with the Cauchy scale factor ($\lambda 2 = 4$), see Figure 6.

Figure 7 shows the maximum principal strain distribution (E1) in the full-scale models (FSM) related to a displacement level equal to 80 mm, according to the correlation between displacement and strain levels provided by the Cauchy law ($\lambda = 2$).

Figure 7 clearly shows that the strain concentration in WALL 0 is higher if compared to WALL 1 and WALL 2 strain patterns. Façade and inner corners appear to be the areas experiencing more significant damages. Moreover, the application of reinforcing elements in WALL 1 and WALL 2 resulted in a reduction of strain levels in the aforementioned areas of the walls. Overall, it is possbile to say that the outcomes of the full scale models are consistent to the numerical results of the reduced scale prototypes.

3   Conclusions

This paper presents the results of numerical analyses carried out in order to simulate the out-of-plane behaviour of stone masonry walls prototypes built with earthquake resistant technique and tested by means of an airbag simulating the seismic load.

The numerical models, prepared using a FE macro-model approach, were calibrated with the results of the experimental tests (sonic and dynamic). The numerical pushover curves obtained from the numerical analyses showed a good correlation with the force-displacement envelopes obtained from the out-of-plane tests. A good correlation was also obtained in terms of maximum load capacity, stiffness, deformation and damage pattern. WALL 1 and WALL 0 post peak behaviour showed a slight difference if compared to the experimental data, whereas WALL 2 post peak behaviour appeared more accurately captured.

In order to assess the overall performances of the reinforcing elements, numerical simulation have been carried out using full-scale models and taking into account the Cauchy scale factors.

To conclude, it can be said that this work highlights the importance of a good characterization of the walls typology to correctly understand their structural behaviour. Moreover, the strategy applied to realize the models of the tested prototypes (FE macro-modelling approach) proved to be a valuable tool in practice-oriented engineering analyses and a good compromise between results accuracy and computational efficiency.

Acknowledgements

References

[1] Roca, P.; Cervera, M.; Gariup, G.; Pelà, L. – "Structural Analysis of Masonry Historical Constructions – Classical and Advanced Approaches", *Arch Comput Methods Eng*, 299-325 July 2010.

[2] Ferreira, T.M.; Costa, A.; Costa, A. – "Analysis of the Out-Of-Plane Seismic Behavior of Unreinforced Masonry: A Literature Review", *International Journal of Architectural Heritage*, pp. 949-972, November 2014.

[3] Lourenço, P. – "Recent advances in Masonry modelling: micromodelling and homogenisation", in *Multiscale Modeling in Solid Mechanics: Computational Approaches*, London, Imperial College Press, 2009, pp. 251-294.

[4] Maccarini, H.; Vasconcelos, G.; Rodrigues, H.; Ortega, J.; Lourenço, P.B. – "Out-of-plane behavior of stone masonry walls: Experimental and numerical analysis", *Construction and Building Materials*, pp. 430-452, 2018.

[5] Murano, A.; Vasconcelos, G.; Rodrigues, H.; Ortega, J. – "Out-of-plane behaviour of stone masonry walls built with earthquake resistant techniques: Experimental characterization", in 11.° Congresso Nacional de Sismologia e Engenharia Sismica, Lisbon, 2019.

[6] DIANA – Finite Element Analysis, DIsplacement method ANalizer. User's Manual, release 10.2, Delft, The Netherlands: DIANA FEA BV, 2017.

[7] Ortega, J. – PhD Thesis, Guimaraes: University of Minho, 2018.

[8] Karanikoloudis, G.; Lourenço, P. – "Seismic assessment of Kuño Tambo Church (Perù): strengthening proposal", University of Minho, Guimaraes (Portugal), 2016.

[9] Lourenço, P.B. – "Masonry Modeling," in *Encyclopedia of Earthquake Engineering*, Berlin, Springer Berlin Heidelberg, 2015, pp. 1-13.

[10] Tomazevic, M. – *Earthquake-Resistant Design of Masonry Buildings*, London: Imperial College Press, 1999.